JVI Journals.ASM.org

Ebola Virus Disease in Mice with Transplanted Human Hematopoietic Stem Cells

Anja Lüdtke,[a,b,c] Lisa Oestereich,[b,c] Paula Ruibal,[a,b,c] Stephanie Wurr,[b,c] Elisa Pallasch,[b,c] Sabrina Bockholt,[b,c] Wing Hang Ip,[a] Toni Rieger,[b,c] Sergio Gómez-Medina,[a] Carol Stocking,[a] Estefanía Rodríguez,[a] Stephan Günther,[b,c] César Muñoz-Fontela[a,b,c]

Heinrich Pette Institute, Leibniz Institute for Experimental Virology, Hamburg, Germany[a]; Bernhard Nocht Institute for Tropical Medicine, Hamburg, Germany[b]; German Centre for Infection Research (DZIF), Partner Site Hamburg, Hamburg, Germany[c]

The development of treatments for Ebola virus disease (EVD) has been hampered by the lack of small-animal models that mimick human disease. Here we show that mice with transplanted human hematopoetic stem cells reproduce features typical of EVD. Infection with Ebola virus was associated with viremia, cell damage, liver steatosis, signs of hemorrhage, and high lethality. Our study provides a small-animal model with human components for the development of EVD therapies.

Ebola virus disease (EVD) is a highly lethal viral syndrome characterized by fever, viremia, multiorgan failure, and, in some cases, bleeding (1). The magnitude of the current EVD outbreak in West Africa has highlighted the need for specific medical countermeasures against EVD (2), but the lack of small-animal models of disease has precluded preclinical testing of therapies. Inbred laboratory mice are resistant to infection with nonadapted Ebola virus (EBOV) and are susceptible only to mouse-adapted EBOV (maEBOV) injected intraperitoneally (i.p.) (3, 4). However, maEBOV infection does not reproduce human EVD pathogenesis unless mouse genetic diversity is increased via systematic crossing of inbred strains (5). Alternatively, mice with deficient innate immunity, such as type I interferon receptor knockout (IFNAR$^{-/-}$) or STAT-1 knockout, are susceptible to both EBOV and maEBOV by several routes, but these mice cannot serve to translate basic findings to human disease due to the lack of a competent immune system (3). In this study, we sought to develop a small-animal model with human hematopoietic cells susceptible to nonadapted EBOV.

Severely immunodeficient mice, such as nonobese diabetic (NOD)/severe combined immunodeficiency (*scid*)/interleukin-2 (IL-2) receptor-γ chain knockout (NSG) mice, allow long-term engraftment of human tissues due to the lack of mature T and B cells (6). In addition, NSG mice are deficient for several high-affinity receptors for cytokines, including IL-2, IL-4, IL-7, IL-9, IL-15, and IL-21, that block the development of natural killer (NK) cells and further impair host innate immunity (6, 7). Previous studies have demonstrated the suitability of NSG mice as a small-animal model for human viral infections, including infections with HIV, Epstein-Barr virus (EBV), influenza virus, and dengue virus (8–11).

To reconstitute the human hematopoietic system in NSG-A2 mice, we utilized the NOD.Cg-*Prkdc*^{scid} *Il2rg*^{tm1Wjl} Tg (HLA-A2.1) 1Enge/SzJ mouse strain from Jackson Laboratories. These mice were kept in individually ventilated cages inside the biosafety level 4 (BSL4) laboratory at the Bernhard Nocht Institute in Hamburg, Germany, and fed with autoclaved food and water. Human CD34$^+$ hematopoietic stem cells (HSCs) were purified from umbilical cord blood of HLA-A2$^+$ donors using a Ficoll gradient and subsequent positive antibody selection (StemSep human CD34 positive selection cocktail; Stem Cell Technologies). All patients agreed to donation of biological material by informed written consent under a protocol approved by the local ethics committee, and all animal experiments were conducted according to the guidelines of the German animal protection law. Four- to 5-week-old female mice were conditioned by sublethal irradiation (240 cGy), and 3 to 4 h later, we transplanted 10^6HSCs/mouse via intravenous injection (retro-orbital). Eight to 12 weeks posttransplantation, peripheral blood, spleen, and bone marrow samples were tested for the presence of human hematopoietic cells using the panleukocyte marker CD45. All organs and blood were processed to obtain single-cell suspensions and were depleted of red blood cells by using commercial lysing buffer (Biolegend). Then, the percentage of human and mouse hematopoietic cells for each organ was determined by flow cytometry, using anti-human CD45 (clone HI30; Biolegend) and anti-mouse CD45 (clone 30-F11; Biolegend) antibodies.

We observed a high level of engraftment of human hematopoietic cells in both lymphoid tissues (40 to 80%) and peripheral tissues (10 to 40%) with the presence of fully differentiated human lymphocytes (T, B, NK, and NKT cells) and myeloid cells (monocytes, granulocytes, and dendritic cells) (data not shown). While the frequencies of these populations differed between experiments, all the human cell subsets were consistently observed in mice with transplanted HSCs. These data demonstrate that humanized NSG-A2 [(hu)NSG-A2] mice develop all cell components of a fully functional adaptive human immune system, in agreement with previous reports (9–11).

Received 9 December 2014 **Accepted** 2 February 2015

Accepted manuscript posted online 11 February 2015

Citation Lüdtke A, Oestereich L, Ruibal P, Wurr S, Pallasch E, Bockholt S, Ip WH, Rieger T, Gómez-Medina S, Stocking C, Rodríguez E, Günther S, Muñoz-Fontela C. 2015. Ebola virus disease in mice with transplanted human hematopoietic stem cells. J Virol 89:4700–4704. doi:10.1128/JVI.03546-14.

Editor: A. García-Sastre

Address correspondence to César Muñoz-Fontela, cesar.munoz-fontela@hpi.uni-hamburg.de.

A.L. and L.O. contributed equally to this work.

doi:10.1128/JVI.03546-14

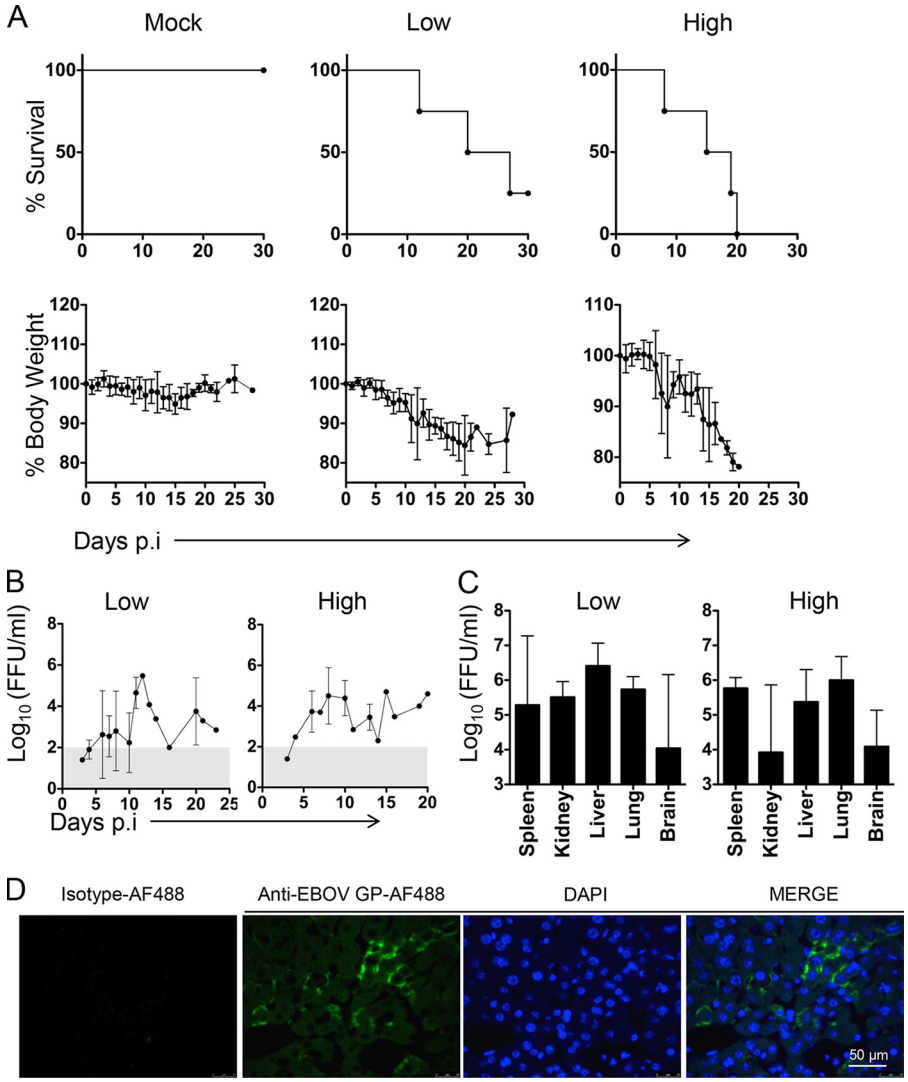

FIG 1 Course of EVD in huNSG-A2 mice. (A) Mice were infected with 1,000 FFU of Ebola virus (EBOV) i.p. and monitored daily over the course of the disease. Kaplan-Meier survival curves and percentage of body weight (mean value ± standard deviation [SD]) are shown. Mice with high levels of HSC engraftment showed more than 40% of human hematopoietic cells (human $CD45^+$) out of the total peripheral blood leukocytes ($n = 4$). Mice with low levels of HSC engraftment showed 20 to 40% of human $CD45^+$ cells of the total peripheral blood leukocytes ($n = 4$), and mock mice showed engraftment with 20 to 40% of human $CD45^+$ cells and received PBS ($n = 4$). (B) Viremia was determined in peripheral blood by an immunofocus assay. Briefly, Vero-E6 cells were incubated with serial dilutions of blood and overlaid with agar to allow plaque formation. Virus foci were revealed at day 7 postinfection by virus-specific antibodies and a secondary fluorescent conjugate. (C) The same protocol as that described for panel B was applied to determine infectious virus in supernatants from homogenized tissues. The range of viremia below the limit of detection of the immunofocus assay is shaded in gray. Graphs represent mean values ± SDs. (D) Immunofluorescence of liver sections showing staining of EBOV glycoprotein (GP) in mouse hepatocytes at day 12 postinfection. Paraffin-embedded tissue sections were deparaffinized in xylene and decreasing concentrations of ethanol before rehydration in PBS. Antigen retrieval was achieved by boiling samples in sodium citrate buffer (pH 6). Sections were then allowed to cool down and were blocked in Tris-buffered saline–BG buffer (TBS-BG; BG is 5% [wt/vol] bovine serum albumin and 5% [wt/vol] glycine) for 2 h. For staining of EBOV-infected cells, a 1:1 mix of two monoclonal antibodies (clones 5D2 and 5E6) were conjugated with Alexa Fluor 488 using an antibody labeling kit (Molecular Probes). AF488-conjugated IgG2a isotype was utilized as a control. A 1:100 dilution of AF488-conjugated Ebola antibody (anti-EBOV GP-AF488) or an isotype dilution was prepared in TBS-BG buffer, and samples were incubated for 1 h at room temperature. DAPI (4′,6-diamidino-2-phenylindole) was used for staining nuclei (1:1,000 dilution). Sections were then washed three times with TBS-BG and mounted in Glow medium (Energene). Digital images were acquired using a DMRB fluorescence microscope (Leica) and a charge-coupled device camera (Diagnostic Instruments). Images were processed in ImageJ.

To test the susceptibility of huNSG-A2 mice to EBOV infection, we inoculated 1,000 focus-forming units (FFU) of EBOV (Ebola virus H.sapiens-tc/COD/1976/Yambuku-Mayinga) i.p. into mice with either low-level engraftment (20 to 40%) or high-level engraftment (>40%) of human hematopoietic cells in peripheral blood leukocytes. A mock group of mice with transplanted HSCs that received phosphate-buffered saline (PBS) was kept as a negative control. All EBOV-infected mice showed a marked weight loss starting around day 7 postinfection (Fig. 1A). By day 20, 50% of mice with low-level engraftment succumbed to EVD while the infection was lethal for 100% of mice with high-level engraftment. These results indicate that the severity of EBOV infection in huNSG-A2 mice was directly correlated with the level of engraftment of human hematopoietic cells.

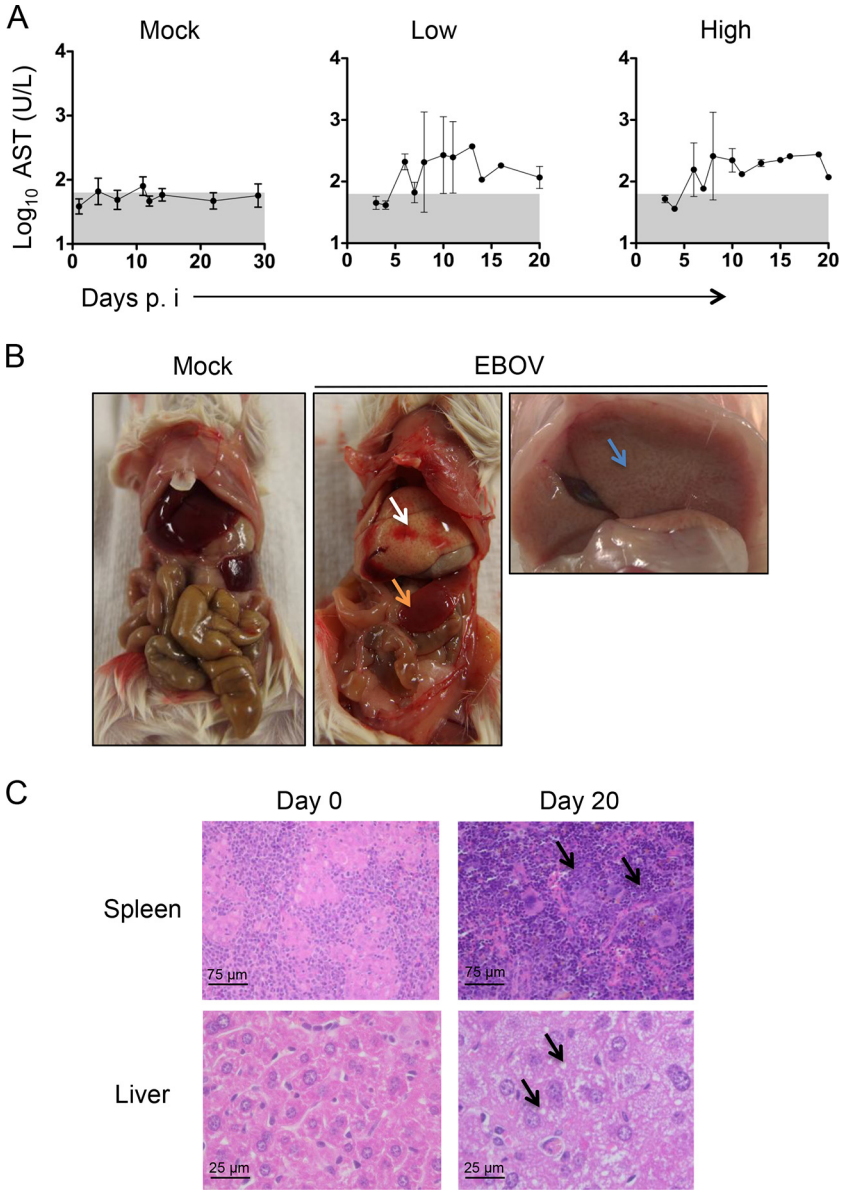

FIG 2 Pathological findings in EBOV-infected huNSG-A2 mice. (A) Serum AST levels were determined by using commercially available colorimetric assay kits (Reflotron, Roche Diagnostics, Germany). The range of AST levels that were below the limit of detection of the assay is shaded in gray. Graphs represent mean values ± SDs. (B) Necropsies were performed in severely ill mice according to the guidelines of our approved animal protocols, which included euthanasia when body weight dropped below 75% of the original weight. The left panel shows a mock-infected control. The middle panel shows an EBOV-infected mouse. The white arrow indicates an area of focal hemorrhage in the liver. The orange arrow indicates splenomegaly. Steatosis (fatty liver) is shown in the right panel (blue arrow). (C) Mouse tissues were fixed in 4% formalin and embedded in paraffin. Sections were stained with hematoxilin and eosin. Black arrows in the upper panel (spleen) indicate areas of strong lymphocytic infiltration. Black arrows in the lower panel (liver) indicate areas of small lipid droplet deposits.

The time of death reflected the incubation period and the course of EVD observed in humans (1).

A common characteristic of EVD in humans is high viremia and virus dissemination to peripheral organs, which is negatively correlated with disease outcome (1, 12). In mice with both low and high levels of engraftment, we observed infectious virus in blood at titers up to 10^5 FFU/ml at the peak of disease (Fig. 1B). In addition, both groups of mice showed the presence of infectious virus in peripheral organs such as kidney, liver, lung, and brain (Fig. 1C). Interestingly, the viral titers were similar in both groups of mice, with liver and lung supporting high viral loads (Fig. 1C), which suggested that cells of mouse origin could support EBOV replication. This hypothesis was confirmed by immunofluorescence analysis of tissue sections using Alexa Fluor 488-conjugated anti-EBOV glycoprotein (GP) antibodies, a kind gift from Gary Kobinger, Public Health Agency of Canada, which revealed the presence of infected cells of mouse origin, such as liver hepatocytes (Fig. 1D). These findings strongly suggest that the higher susceptibility to lethal infection observed in mice with a high level of engraftment of human cells may be related to immunopathology rather than the presence of a higher number of human

target cells for the virus, in agreement with findings in other EVD models such as nonhuman primates (NHPs) (13).

Next, we sought to evaluate the pathogenesis of EVD in huNSG-A2 mice. First we determined the serum levels of aspartate aminotransferase (AST) in EBOV-infected mice as an indication of cell damage (13). In mice with both low and high levels of HSC engraftment, we observed elevation of AST levels in serum over the course of disease, which mimicked findings in NHPs and human patients (1, 13–15) (Fig. 2A). Strikingly, assessment of gross pathology during necropsies indicated liver steatosis (fatty liver) in EBOV-infected mice (Fig. 2B), which was confirmed by visualization of small-droplet steatosis in tissue sections (Fig. 2D). Mild to moderate fatty liver is a common observation in postmortem examination of liver tissues from EBOV-infected NHPs and humans (16, 17) and to our knowledge has never been reproduced before in a mouse model of EVD. In one out of six necropsies performed, we also observed areas of focal hemorrhage and necrosis in the livers of EBOV-infected mice (Fig. 2B). Thus, our mouse model may also reproduce EBOV-associated bleeding disorders that are associated with EVD in a small percentage of human patients (1, 18). Necropsies also revealed clear signs of splenomegaly, a pathological finding previously reported in filovirus-infected NHPs (Fig. 2B) (19). The evaluation of histopathological features confirmed the necropsy findings that showed extensive lymphocyte infiltrates in spleen and lipid droplet deposits in the livers of EBOV-infected mice (Fig. 2C). Taken together, our results indicate that huNSG-A2 mice reproduce the pathological features of EVD in humans and NHPs, including liver damage, bleeding, and immunopathology.

To specifically determine the role of human hematopoietic cells in our system, we established two additional infection models. First, we utilized NSG-A2 mice without HSC transplantation, and second, we reconstituted the hematopoietic system in NSG-A2 mice with mouse bone marrow progenitor cells from C57BL/6 donor mice (moNSG-A2) (Fig. 3A). These moNSG-A2 mice developed a fully differentiated mouse hematopoietic system (data not shown). NSG-A2 mice without HSC transplantation showed only mild signs of disease until the third week postinfection, at which time they showed gradual weight loss until the time of death (Fig. 3A). These results suggested a lengthy disease similar to that of *scid* mice infected with Marburg virus (20). This hypothesis was further confirmed with the observation of long-term unresolved viremia in these mice, which was consistent with lack of virus clearance mechanisms (Fig. 3B). Serum levels of AST also increased gradually in these mice until the time of death (Fig. 3B). Conversely, all moNSG-A2 mice survived EBOV infection, mimicking observations in wild-type inbred mice infected with nonadapted filoviruses (3). Interestingly, moNSG-A2 mice showed weight loss up to day 10 postinfection, which coincided with low levels of viremia and a transient elevation of AST (Fig. 3A and B). These results probably reflect the importance of innate immune responses for early control of EBOV replication, which are impaired in the nonhematopoietic compartment of moNSG-A2 mice (4, 21). The difference in EBOV virulence between moNSG-A2 mice and huNSG-A2 mice indicates the important role of human hematopoietic cells for pathogenesis in our model.

To the best of our knowledge, this study provides for the first time a small-animal model with a human hematopoietic system that recapitulates some of the main features of EVD pathogenesis, namely, viremia, cell and organ damage, and high lethality. We have also been able to reproduce these findings in huNSG-A2 mice infected intranasally (data not shown), suggesting susceptibility to nonadapted EBOV by several infection routes. Due to the functional HLA-A2-restricted CD8 T-cell responses observed in these mice in other viral infections (10, 11), we anticipate that our model will provide insight into not only the pathogenesis but also the correlates of immune protection against EBOV. Importantly,

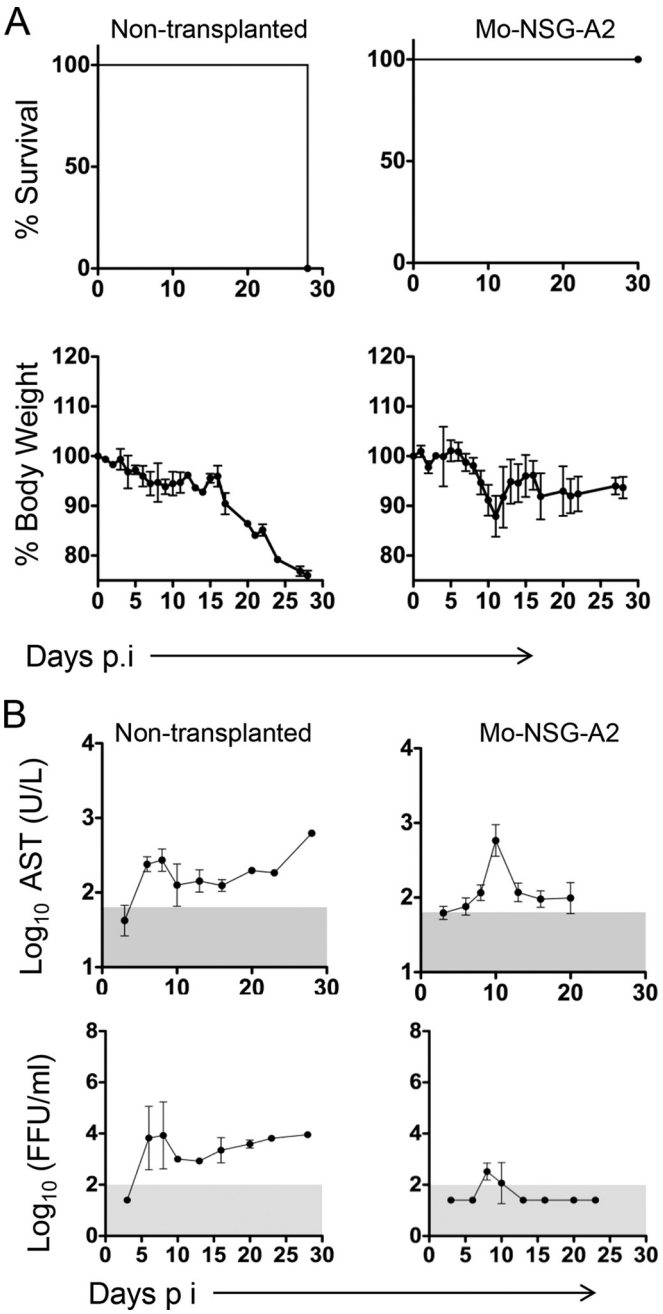

FIG 3 Course of EVD in NSG mice without HSC transplantation and mouse bone marrow controls. (A) Kaplan-Meier survival curves and percentage of body weight are shown. Mice without HSC transplantation ($n = 2$) and moNSG-A2 mice ($n = 4$) were infected with 1,000 FFU of EBOV i.p. (B) AST levels in serum and viremia were determined as described in the legend to Fig. 2. Gray areas indicate the limit of detection of the assays. Graphs throughout the figure represent mean values ± SDs.

we were able to observe signs of liver steatosis and hemorrhage, features of EVD in humans whose relevance in the disease is not well understood (1, 17, 18). We speculate that the presence of human macrophages, which are involved in both inflammation-associated fatty liver and disseminated intravascular coagulation (22, 23), may be responsible for these findings. Further optimization of the model via depletion of residual mouse macrophages (24) might help to further test this hypothesis. We expect that our model will serve to accelerate preclinical development of EBOV vaccines and antivirals and to determine correlates of immune protection against EVD in humans.

ACKNOWLEDGMENTS

We thank Ulla Müller, Gundula Pilnitz-Stolze, and Rui Qiao for excellent technical support. We also thank Gary Kobinger for the monoclonal antibodies against EBOV GP.

This work was partially funded by a German Center of Infection Research (DZIF)-EBOCON grant to C. M.-F. and S.G. A.L. is a recipient of a predoctoral fellowship from the Leibniz Center of Infection. The Heinrich-Pette-Institute is financed by the German Federal Ministry of Health and the Freie und Hansestadt Hamburg.

None of the authors have any conflict of interest related with this study.

REFERENCES

1. **Schieffelin JS, Shaffer JG, Goba A, Gbakie M, Gire SK, Colubri A, Sealfon RSG, Kanneh L, Moigboi A, Momoh M, Fullah M, Moses LM, Brown BL, Andersen KG, Winnicki S, Schaffner SF, Park DJ, Yozwiak NL, Jiang P-P, Kargbo D, Jalloh S, Fonnie M, Sinnah V, French I, Kovoma A, Kamara FK, Tucker V, Konuwa E, Sellu J, Mustapha I, Foday M, Yillah M, Kanneh F, Saffa S, Massally JLB, Boisen ML, Branco LM, Vandi MA, Grant DS, Happi C, Gevao SM, Fletcher TE, Fowler RA, Bausch DG, Sabeti PC, Khan SH, Garry RF, the KGH Lassa Fever Program, the Viral Hemorrhagic Fever Consortium, and the WHO Clinical Response Team.** 2014. Clinical illness and outcomes in patients with Ebola in Sierra Leone. N Engl J Med **371:**2092–2100. http://dx.doi.org/10.1056/NEJMoa1411680.
2. **Frieden TR, Damon I, Bell BP, Kenyon T, Nichol S.** 2014. Ebola 2014—new challenges, new global response and responsibility. N Engl J Med **371:**1177–1180. http://dx.doi.org/10.1056/NEJMp1409903.
3. **Bray M.** 2001. The role of the type I interferon response in the resistance of mice to filovirus infection. J Gen Virol **82:**1365–1373.
4. **Bradfute SB, Warfield KL, Bray M.** 2012. Mouse models for filovirus infections. Viruses **4:**1477–1508. http://dx.doi.org/10.3390/v4091477.
5. **Rasmussen AL, Okumura A, Ferris MT, Green R, Feldmann F, Kelly SM, Scott DP, Safronetz D, Haddock E, LaCasse R, Thomas MJ, Sova P, Carter VS, Weiss JM, Miller DR, Shaw GD, Korth MJ, Heise MT, Baric RS, de Villena FP-M, Feldmann H, Katze MG.** 2014. Host genetic diversity enables Ebola hemorrhagic fever pathogenesis and resistance. Science **346:**987–991. http://dx.doi.org/10.1126/science.1259595.
6. **Ishikawa F, Yasukawa M, Lyons B, Yoshida S, Miyamoto T, Yoshimoto G, Watanabe T, Akashi K, Shultz LD, Harada M.** 2005. Development of functional human blood and immune systems in NOD/SCID/IL2 receptor γ chain^{null} mice. Blood **106:**1565–1573. http://dx.doi.org/10.1182/blood-2005-02-0516.
7. **Shultz LD, Brehm MA, Bavari S, Greiner DL.** 2011. Humanized mice as a preclinical tool for infectious disease and biomedical research. Ann N Y Acad Sci **1245:**50–54. http://dx.doi.org/10.1111/j.1749-6632.2011.06310.x.
8. **Shacklett BL.** 2008. Can the new humanized mouse model give HIV research a boost. PLoS Med **5:**e13. http://dx.doi.org/10.1371/journal.pmed.0050013.
9. **Strowig T, Chijioke O, Carrega P, Arrey F, Meixlsperger S, Rämer PC, Ferlazzo G, Münz C.** 2010. Human NK cells of mice with reconstituted human immune system components require preactivation to acquire functional competence. Blood **116:**4158–4167. http://dx.doi.org/10.1182/blood-2010-02-270678.
10. **Yu CI, Gallegos M, Marches F, Zurawski G, Ramilo O, García-Sastre A, Banchereau J, Palucka AK.** 2008. Broad influenza-specific CD8+ T-cell responses in humanized mice vaccinated with influenza virus vaccines. Blood **112:**3671–3678. http://dx.doi.org/10.1182/blood-2008-05-157016.
11. **Jaiswal S, Pearson T, Friberg H, Shultz LD, Greiner DL, Rothman AL, Mathew A.** 2009. Dengue virus infection and virus-specific HLA-A2 restricted immune responses in humanized NOD-*scid IL2rγ*^{null} mice. PLoS One **4:**e7251. http://dx.doi.org/10.1371/journal.pone.0007251.
12. **Baize S, Leroy EM, Georges-Courbot MC, Capron M, Lansoud-Soukate J, Debré P, Fisher-Hoch SP, McCormick JB, Georges AJ.** 1999. Defective humoral responses and extensive intravascular apoptosis are associated with fatal outcome in Ebola virus-infected patients. Nat Med **5:**423–426. http://dx.doi.org/10.1038/7422.
13. **Feldmann H, Geisbert TW.** 2011. Ebola haemorrhagic fever. Lancet **377:**849–862. http://dx.doi.org/10.1016/S0140-6736(10)60667-8.
14. **Bente D, Gren J, Strong JE, Feldmann H.** 2009. Disease modeling for Ebola and Marburg viruses. Dis Model Mech **2:**12–17. http://dx.doi.org/10.1242/dmm.000471.
15. **Ebihara H, Rockx B, Marzi A, Feldmann F, Haddock E, Brining D, LaCasse RA, Gardner D, Feldmann H.** 2011. Host response dynamics following lethal infection of rhesus macaques with Zaire ebolavirus. J Infect Dis **204**(Suppl 3)**:**S991–S999. http://dx.doi.org/10.1093/infdis/jir336.
16. **Alves DA, Glynn AR, Steele KE, Lackemeyer MG, Garza NL, Buck JG, Mech C, Reed DS.** 2010. Aerosol exposure to the Angola strain of Marburg virus causes lethal viral hemorrhagic fever in cynomolgus macaques. Vet Pathol **47:**831–851. http://dx.doi.org/10.1177/0300985810378597.
17. **Martines RB, Ng DL, Greer PW, Rollin PE, Zaki SR.** 2015. Tissue and cellular tropism, pathology and pathogenesis of Ebola and Marburg viruses. J Pathol **235:**153–174. http://dx.doi.org/10.1002/path.4456.
18. **McElroy AK, Erickson BR, Flietstra TD, Rollin PE, Nichol ST, Towner JS, Spiropoulou CF.** 2014. Ebola hemorrhagic fever: novel biomarker correlates of clinical outcome. J Infect Dis **210:**558–566. http://dx.doi.org/10.1093/infdis/jiu088.
19. **Jahrling PB, Geisbert TW, Jaax NK, Hanes MA, Ksiazek TG, Peters CJ.** 1996. Experimental infection of cynomolgus macaques with Ebola-Reston filoviruses from the 1989-1990 U.S. epizootic. Arch Virol Suppl **11:**115–134.
20. **Warfield KL, Alves DA, Bradfute SB, Reed DK, VanTongeren S, Kalina WV, Olinger GG, Bavari S.** 2007. Development of a model for marburgvirus based on severe-combined immunodeficiency mice. Virol J **4:**108. http://dx.doi.org/10.1186/1743-422X-4-108.
21. **Ebihara H, Takada A, Kobasa D, Jones S, Neumann G, Theriault S, Bray M, Feldmann H, Kawaoka Y.** 2006. Molecular determinants of Ebola virus virulence in mice. PLoS Pathog **2:**e73. http://dx.doi.org/10.1371/journal.ppat.0020073.
22. **Geisbert TW, Young HA, Jahrling PB, Davis KJ, Kagan E, Hensley LE.** 2003. Mechanisms underlying coagulation abnormalities in Ebola hemorrhagic fever: overexpression of tissue factor in primate monocytes/macrophages is a key event. J Infect Dis **188:**1618–1629. http://dx.doi.org/10.1086/379724.
23. **Weisberg SP, Hunter D, Huber R, Lemieux J, Slaymaker S, Vaddi K, Charo I, Leibel RL, Ferrante AW.** 2006. CCR2 modulates inflammatory and metabolic effects of high-fat feeding. J Clin Invest **116:**115–124. http://dx.doi.org/10.1172/JCI24335.
24. **Hu Z, van Rooijen N, Yang Y-G.** 2011. Macrophages prevent human red blood cell reconstitution in immunodeficient mice. Blood **118:**5938–5946. http://dx.doi.org/10.1182/blood-2010-11-321414.